Proceedings of the 48th International School and Conference on the Physics of Semiconductors "Jaszowiec 2019"

Structural and Optical Properties of GaSe/GaAs(001) Layers Grown by Molecular Beam Epitaxy

P.S. Avdienko*, S.V. Sorokin, I.V. Sedova, D.A. Kirilenko, A.N. Smirnov, I.A. Eliseev, V.Yu. Davydov and S.V. Ivanov

Ioffe Institute, 26 Politekhnicheskaya, 194021 St. Petersburg, Russia

This paper reports on molecular beam epitaxy of GaSe 2D-layers on GaAs(001) substrates at growth temperatures of $T_S \approx 400$–$540\,^\circ$C as well as studies of their structural and optical properties. Transmission electron microscopy and the Raman spectroscopy techniques have established a correlation between the molecular beam epitaxy growth conditions and the GaSe polytypes being formed. It has been shown that GaSe layers grown at $T_S \approx 400\,^\circ$C can be characterized as a γ-GaSe polytype with a rhombohedral crystal lattice structure, whereas the layers grown at $T_S \approx 500\,^\circ$C have a hexagonal structure and possess a ε-GaSe polytype. The latter also exhibit strong near band-edge photoluminescence at $T = 300$ K. The strong anisotropy of the photoluminescence intensity in an array of GaSe nanoplatelets has been revealed.

DOI: 10.12693/APhysPolA.136.608

PACS/topics: 81.15.Hi, 68.37.Lp, 68.37.Hk, 61.46.–w, 61.82.Fk, 78.30.–j

1. Introduction

The development of epitaxial growth techniques of layered materials (MoS_2, WSe_2, GaSe, etc.) is of great importance due to a large number of their potential applications. In particular, GaSe is a promising material for the fabrication of field-effect transistors, terahertz generators, and high-efficient photodetectors [1]. The strong anisotropy of the transport, mechanical, and optical properties of GaSe is a consequence of its layered crystal structure. Bulk GaSe crystals consist of vertically ordered ≈ 0.8 nm-thick layers which are bonded together by weak van der Waals forces, and each GaSe layer contains four covalently-bonded Se–Ga–Ga–Se atomic sheets [2]. GaSe thin films are generally fabricated by mechanical or chemical exfoliation techniques. However, in order to realize practical applications of the 2D material-based devices, it is important to synthesize large-area, high-quality 2D crystals on commercially available substrates. This paper reports on structural and optical properties of GaSe layers grown by molecular beam epitaxy (MBE) on GaAs(001) substrates.

2. Experiment

GaSe layers were grown on epiready GaAs(001) substrates at a substrate temperature of $T_S = 400$–$540\,^\circ$C by using a double-chamber MBE setup (SemiTEq, Russia). The Se/Ga flux ratio was controlled by measuring the Se and Ga beam equivalent pressures (BEPs) at the substrate position by using a Bayard–Alpert ion gauge. A standard Ga effusion cell as well as a Se valve cracking cell (Veeco, US) with the cracking zone temperature of $T_{\mathrm{Se(cr)}} = 500\,^\circ$C were used as molecular beams sources. Prior to the growth, the substrates were heated in the growth chamber at $T_S \approx 580$–$600\,^\circ$C in the absence of As flux to remove the surface oxide layer, which was controlled by reflection high energy electron diffraction (RHEED) measurements. The details of the MBE growth of GaSe/GaAs(001) layers were published elsewhere [3].

The samples were characterized by cross-sectional transmission electron microscopy (TEM) (JEOL JEM 2100F microscope), scanning electron microscopy (SEM) (CamScan microscope), Raman spectroscopy, and microphotoluminescence spectroscopy (μ-PL) techniques. The Raman and μ-PL measurements were performed at room temperature using a T64000 (Horiba Jobin-Yvon) spectrometer equipped with a confocal microscope. The line at 532 nm (2.33 eV) of Nd:YAG laser (Torus, Laser Quantum, Inc.) was used as the excitation source. The laser power on the sample was as low as ≈ 25 μW in a spot size of ≈ 1 μm.

3. Results and discussion

GaSe films can crystallize in different polytypes (β, ε, γ, and δ), which differ from each other by stacking sequence of the layers [2]. γ-GaSe has a rhombohedral crystal lattice with the $R3m$ space group, whereas β, ε, and δ-GaSe have a hexagonal crystal lattice with $P6_3/mmc$, $P\bar{6}m2$, and $P6_3mc$ space groups, respectively. The formation of one or another polytype depends on the method of preparation as well as growth conditions (see, e.g. [4]). In particular, GaSe layers grown by MBE are usually of ε- or γ-polytype [5–7].

The influence of MBE growth conditions (Se/Ga flux ratio, Ga flux intensity) on the surface morphology of GaSe/GaAs(001) layers has been studied by using the SEM technique [3]. The surface morphology of the samples grown at low growth temperature ($T_S \approx 400\,^\circ$C) and

*corresponding author

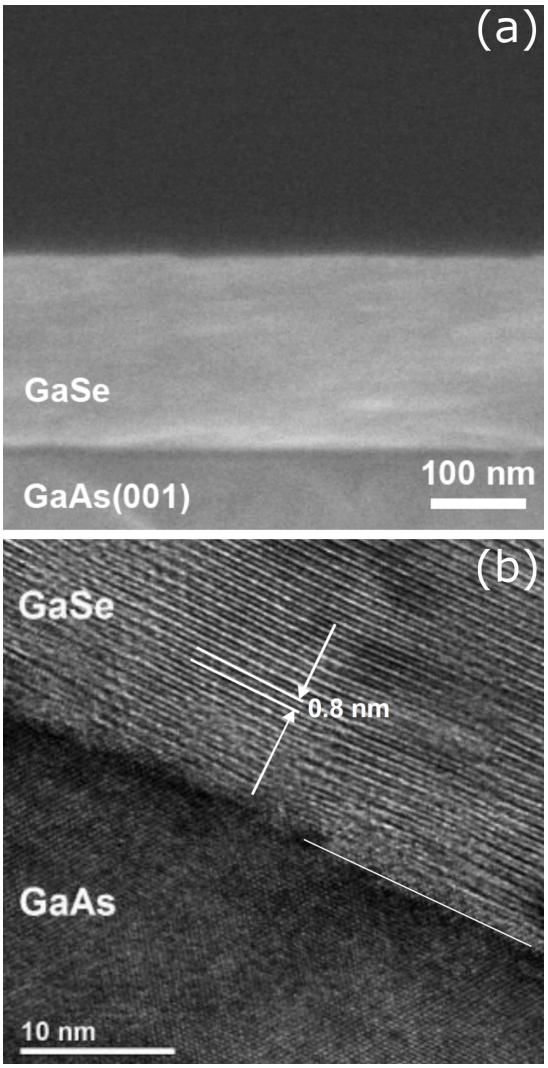

Fig. 1. Cross-sectional SEM (a) and TEM (b) images of the GaSe layer grown on a GaAs(001) substrate at $T_S \approx 400\,^{\circ}\mathrm{C}$ (Se/Ga (BEP) flux ratio ≈ 36).

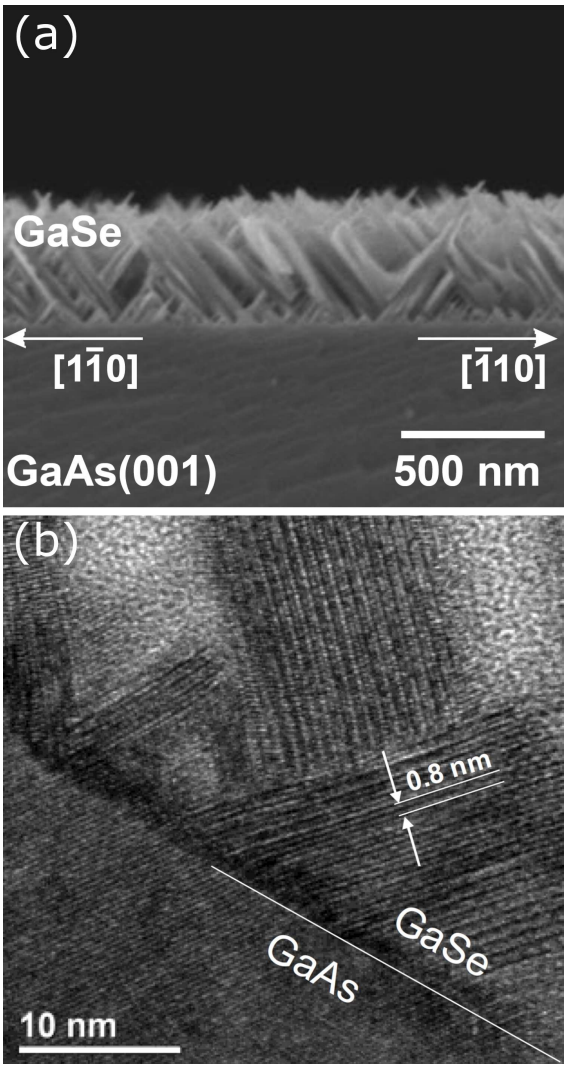

Fig. 2. Cross-sectional SEM (a) and TEM (b) images of the GaSe layers grown on a GaAs(001) substrate at $T_S = 500\,^{\circ}\mathrm{C}$ (Se/Ga (BEP) flux ratio ≈ 22).

different Se/Ga flux ratios looks similar. One can see a number of so-called "nanoplatelets" of different sizes and shapes randomly distributed on the relatively flat growth surface. The surface density of nanoplatelets as well as their size slightly decreases with a decrease in the Se/Ga flux ratio [3]. The cross SEM image of the sample grown at $T_S \approx 400\,^{\circ}\mathrm{C}$ demonstrates the formation of a relatively plain layer with nearly abrupt GaSe/GaAs(001) interface (Fig. 1a). The TEM electron diffraction pattern of the same sample indicates that the layer has a predominantly rhombohedral structure and thus corresponds to the γ-polytype. The $\boldsymbol{c}$ axis of the GaSe layer is directed normally to the substrate-layer interface (Fig. 1b).

With increasing T_S the surface morphology of GaSe layers becomes rougher. The density of nanoplatelets on the growth surface also increases significantly. At $T_S > 500\,^{\circ}\mathrm{C}$ the structure consists of a set of nanoplatelets tilted towards both [1$\bar{1}$0] and [$\bar{1}$10] directions of the GaAs substrate (Fig. 2a) [8]. Despite a certain degree of disordering, due to the chemical interaction between the substrate and the growing layer, the $\boldsymbol{c}$ axis of GaSe nanoplatelets is mainly oriented along the ⟨111⟩ directions of the GaAs substrate (Fig. 2b). However, in Fig. 2b one can also see the formation of an intermediate layer near the GaSe/GaAs interface in some nanopletelets, which leads to an additional layer tilt caused by a partial stress relaxation to accommodate the lattice mismatch between GaSe and GaAs, as was observed previously [9]. When the growth temperature is raised up to $T_S > 530$–$540\,^{\circ}\mathrm{C}$, no growth of GaSe has been observed even at a high Ga flux intensity.

Figure 3a presents the Raman spectrum of the bulk ε-GaSe sample (curve 1), produced by HQ *Graphene*, which was obtained in a scattering configuration with the incident light directed along $\boldsymbol{c}$ axis. The figure also shows the typical Raman spectra of GaSe layers grown on GaAs (001) substrate at different growth conditions.

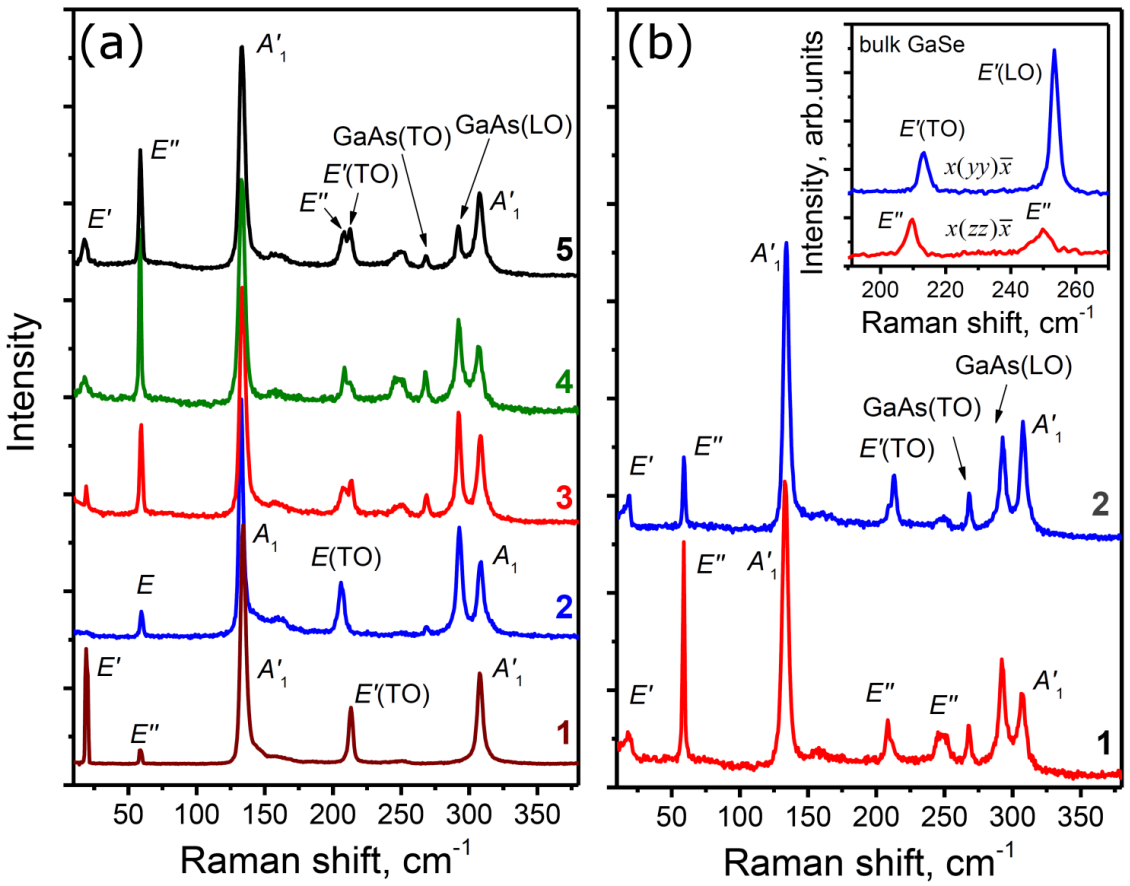

Fig. 3. (a) Raman spectrum of the "bulk" ε-GaSe layer — curve 1. Raman spectra of GaSe layers grown on GaAs(001) substrates at $T_S \approx 400\,^{\circ}$C (curves 2, 5), $T_S \approx 500\,^{\circ}$C (curve 3), and using two-stage mode (curve 4). All spectra are normalized to the intensity of the A_1' symmetry line. (b) The polarized Raman spectra of the sample consisting of an array of GaSe nanoplatelets (see Fig. 2a). The polarization of the incident and scattered light is parallel to either to the $[1\bar{1}0]$ direction (curve 1) or the [110] direction (curve 2) of the substrate. The inset shows the polarized Raman spectra of bulk ε-GaSe.

It is seen that the Raman spectra of MBE grown GaSe layers contain lines corresponding to vibrational modes in GaSe [10], as well as two additional lines at frequencies of 268 and 291 cm^{-1}, caused by light scattering on TO and LO phonons in the GaAs substrate. Curve 2 in Fig. 3a shows the typical Raman spectrum of a GaSe layer grown at $T_S \approx 400\,^{\circ}$C. The main difference between this spectrum and the spectrum of bulk ε-GaSe sample is the absence of a line at a frequency of 19 cm^{-1}. According to the group-theory analysis, the lowest frequency line in the Raman spectrum of GaSe should correspond to interlayer vibrations. However, in the primitive unit cell of γ-GaSe there is only one GaSe layer [12]. Since the adjacent layers belong to different primitive unit cells, the interlayer vibrations refer to the modes at the Brillouin zone boundary and hence should not be observed in the first-order Raman spectra. The absence of a line at a frequency of 19 cm^{-1} in the typical Raman spectrum of the GaSe layer grown at $T_S \approx 400\,^{\circ}$C confirms the conclusion made from TEM data that the sample belongs to the γ-GaSe polytype.

For the layers grown at $T_S \approx 500\,^{\circ}$C (curve 3 in Fig. 3a) the line positions in the Raman spectra are very close to the corresponding lines in the spectrum of the bulk ε-GaSe sample. However, unlike the latter containing only one line near 213 cm^{-1}, a distinct doublet is observed in the spectra of MBE grown samples 3 and 4 in this spectral region. The presence of such a doublet is a consequence of the substantial deviation of the $\boldsymbol{c}$ axis in the GaSe nanoplatelets from the normal to the substrate-layer interface. The Raman data obtained allowed us to assume that these layers predominantly possess ε-polytype.

The GaSe layer grown in a two-stage mode, i.e. with the initial nucleation layer grown at $T_S = 400\,^{\circ}$C, and the main layer grown at $T_S = 500\,^{\circ}$C (curve 4 in Fig. 3a) can also be identified as being of the ε-GaSe polytype. The TEM electron diffraction measurements (not shown here) agree well with this assumption, indicating the hexagonal crystal structure of the grown layer. An additional argument in favor of this interpretation is the first-principle calculations which predict the

ε-polytype being a more stable form in comparison with that of β-polytype, also having a hexagonal crystal structure [11].

Nevertheless, there is no unambiguous correlation between the growth temperature and the formed GaSe polytype. In particular, GaSe layer grown at low $T_S \approx 400\,^{\circ}\mathrm{C}$ with a rough surface morphology (probably due to non-optimum conditions at the initial growth stage) consists predominantly of ε-polytype according to its Raman spectrum (curve 5 in Fig. 3a). The substantial deviation of the $\boldsymbol{c}$ axis from the normal to the substrate plane is also presented in this sample. This allows one to conclude that the formation of one or another polytype in GaSe is determined by a combination of different factors, not only by the growth temperature.

Figure 3b shows the polarized Raman spectra of the sample consisting of an array of GaSe nanoplatelets (see Fig. 2a), which was grown at $T_S = 500\,^{\circ}\mathrm{C}$. The spectra were obtained in two scattering configurations: the polarization of the incident and scattered light was parallel either to the $[1\bar{1}0]$ direction (curve 1) or to the [110] direction (curve 2) of the substrate. The polarized Raman spectra of bulk ε-GaSe obtained in scattering configuration with incident light directed normally to the optical $\boldsymbol{c}$ axis are shown in the inset to Fig. 3b. The pronounced difference in the spectra obtained using $x(zz)\bar{x}$ and $x(yy)\bar{x}$ scattering geometries is clearly seen (here, the z direction is parallel to the optical $\boldsymbol{c}$ axis). Comparative analysis of the polarized Raman spectra obtained for a bulk ε-GaSe and an array of GaSe nanoplatelets allows one to conclude that the array of nanoplatelets is a strictly oriented one. It is established that the projection of the optical $\boldsymbol{c}$ axis in nanoplatelets on the substrate plane is oriented along the $[1\bar{1}0]$ or $[\bar{1}10]$ direction of the GaAs substrate. This finding is fully consistent with the TEM data (Fig. 2b) obtained on the same sample.

GaSe layers grown at high $T_S \approx 500\,^{\circ}\mathrm{C}$ demonstrate strong PL at $T = 300$ K. Figure 4a presents linearly polarized PL spectra of an array of GaSe nanoplatelets in the region of the fundamental absorption edge. The exciting polarized radiation ($h\nu_{\mathrm{exc}} = 2.33$ eV) was incident along the normal to the substrate plane and at an angle of $\alpha = 40$–$45°$ to the optical $\boldsymbol{c}$ axis of nanoplatelets. The emitted light was detected in the opposite direction. In the geometry of the experiment shown in the inset to Fig. 4a the exciting and detected light propagating inside the nanoplatelet contains both polarization components $\boldsymbol{E} \parallel \boldsymbol{c}$ and $\boldsymbol{E} \perp \boldsymbol{c}$. Rotation of the nanoplatelet about *OO'* axis by 90° results in exciting and detecting the nanocrystal PL in pure $\boldsymbol{E} \perp \boldsymbol{c}$ polarization from the same point of the sample. The spectral position (1.99 eV) of the emission bands in Fig. 4a corresponds to the position of the direct free exciton emission band at $T = 300$ K [13]. It is evident that the observed free exciton emission is polarized predominantly within $\boldsymbol{E} \parallel \boldsymbol{c}$.

To explain such a strong anisotropy in the PL intensity, let us consider the structure of the energy levels of free excitons in GaSe. If one includes the spin and

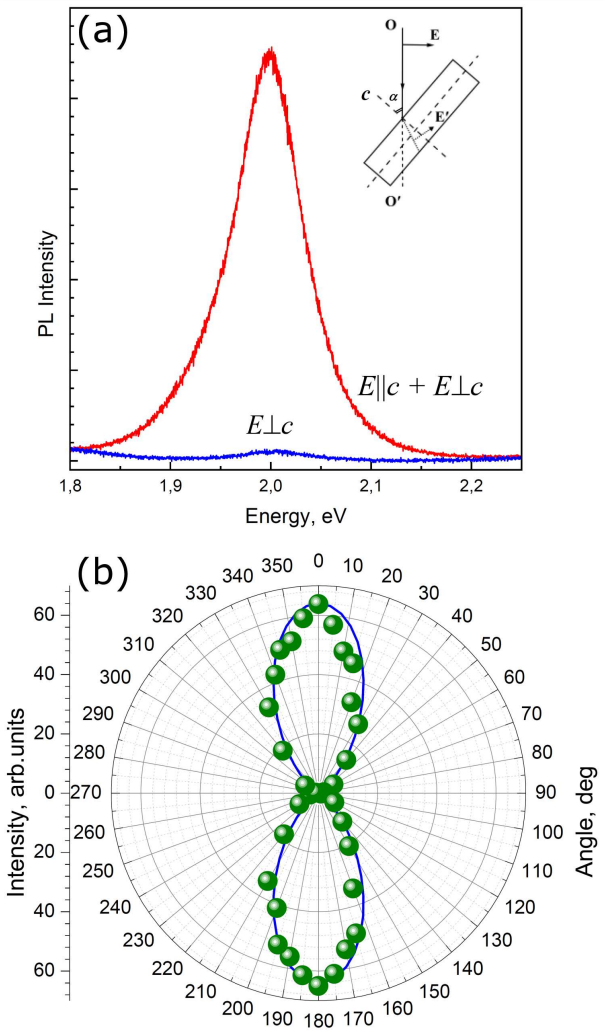

Fig. 4. (a) Room temperature linearly polarized PL spectra of an array of GaSe nanoplatelets in the region of the fundamental absorption edge. (b) The dependence of the PL intensity vs. the angle between the projection of the polarization of light and the projection of the optical $\boldsymbol{c}$ axis of the nanoplatelets on the substrate plane.

electron–hole exchange interaction, the ground state of the direct free exciton in the GaSe crystal (space group $P\bar{6}m2$) splits into singlet (Γ_4) and lower-lying triplet ($\Gamma_6 + \Gamma_3$) states. For a free exciton the singlet-triplet splitting is $\Delta \cong 2$ meV [14]. The $\Gamma_6 - \Gamma_3$ splitting is $\Delta_1 \ll \Delta$. Optical transitions to the singlet state Γ_4 (spin $S = 0$) are allowed in the $\boldsymbol{E} \parallel \boldsymbol{c}$ polarization. Triplet excitons have a total spin $S = 1$, with $S_z = 0, \pm 1$ spin projections on the $\boldsymbol{c}$ axis. Optical transitions to the triplet states Γ_6 with $S_z = \pm 1$ are allowed in the $\boldsymbol{E} \perp \boldsymbol{c}$ polarization due to a weak spin–orbit interaction, and the Γ_3 state with $S_z = 0$ is optically inactive [14]. On the assumption that under band-to-band optical excitation the generation rates of the Γ_4 and Γ_6 excitons are close to each other, as well as the lifetimes of the excitons, their

emission intensities should be proportional to the probabilities of optical transitions from the exciton states to the ground state of the crystal. In this case the ratio of $\approx$ 45–50 between the emission intensities in the $\boldsymbol{E} \parallel \boldsymbol{c}$ and $\boldsymbol{E} \perp \boldsymbol{c}$ polarization should be ascribed to the different probabilities of optical transitions from the singlet (W_s) and triplet (W_t) states, taking into account that $W_s \gg W_t$ [15].

Figure 4b shows the dependence of the PL intensity vs. the angle between the projection of the polarization of light and the projection of the optical $\boldsymbol{c}$ axis of the nanoplatelets on the substrate plane. The angles 0° and 180° correspond to the $\boldsymbol{E} \parallel \boldsymbol{c}$ polarization, and the angles 90° and 270° correspond to the $\boldsymbol{E} \perp \boldsymbol{c}$ polarization. The strong anisotropic dependence of the PL intensity is an additional evidence of a strictly oriented array of GaSe nanoplatelets.

4. Conclusions

GaSe layers grown by MBE on GaAs(001) substrates at substrate temperature within T_S = 400–540 °C range have been studied in detail using a number of characterization techniques. The correlation was established between the MBE growth conditions and GaSe polytype formed. GaSe layers with a relatively flat surface morphology grown at T_S = 400 °C belong to the γ-GaSe polytype with the $\boldsymbol{c}$ axis directed normally to the substrate surface. ε-GaSe polytype dominates in GaSe layers grown at $T_S \approx 500$ °C. The TEM measurements indicate the preferential orientation of the $\boldsymbol{c}$ axis of ε-GaSe along the $\langle 111 \rangle$ directions of the GaAs substrate. GaSe layers grown at high $T_S \approx 500$ °C demonstrate strong near band-edge photoluminescence at T = 300 K. A strong anisotropy of the PL intensity in a strictly oriented array of GaSe nanoplatelets grown at $T_S \approx 500$ °C has been found and explained.

Acknowledgments

The authors are thankful to A.N. Starukhin for the fruitful discussion and valuable comments. TEM characterization was performed in the Joint Research Center "Material science and characterization in advanced technology" with partial financial support from the Ministry of Education and Science of the Russian Federation (project id: RFMEFI62117X0018).

References

[1] D.J. Late, B. Liu, J. Luo, A. Yan, H.S.S. Ramakrishna Matte, M. Grayson, C.N.R. Rao, V.P. Dravid, *Adv. Mater.* **24**, 3549 (2012).

[2] A. Kuhn, A. Chevy, R. Chevalier, *Phys. Status Solidi A* **31**, 469 (1975).

[3] S.V. Sorokin, P.S. Avdienko, I.V. Sedova, D.A. Kirilenko, M.A. Yagovkina, V.Y. Davydov, A.N. Smirnov, S.V. Ivanov, *Semiconductors* **53**, 1131 (2019).

[4] C.D. Blasi, D. Manno, A. Rizzo, *Nuovo Cim. D* **11**, 1145 (1989).

[5] Z.R. Dai, S.R. Chegwidden, L.E. Rumaner, F.S. Ohuchi, *J. Appl. Phys.* **85**, 2603 (1999).

[6] X. Yuan, L. Tang, S. Liu, P. Wang, Z. Chen, C. Zhang, Y. Liu, W. Wang, Y. Zou, C. Liu, N. Guo, J. Zou, P. Zhou, W. Hu, F. Xiu, *Nano Lett.* **15**, 3571 (2015).

[7] C.H. Lee, S. Krishnamoorthy, D.J. O'Hara, M.R. Brenner, J.M. Johnson, J.S. Jamison, R.C. Myers, R.K. Kawakami, J. Hwang, S. Rajan, *J. Appl. Phys.* **121**, 094302 (2017).

[8] N. Kojima, K. Sato, A. Yamada, M. Konagai, K. Takahashi, *Jpn. J. Appl. Phys.* **33**, L1482 (1994).

[9] N. Kojima, K. Sato, M. Budiman, A. Yamada, M. Konagai, K. Takahashi, Y. Nakamura, O. Nittono, *J. Cryst. Growth* **150**, 1175 (1995).

[10] R.M. Hoff, J.C. Irwin, R.M.A. Lieth, *Can. J. Phys.* **53**, 1606 (1975).

[11] A. Polian, K. Kunc, A. Kuhn, *Solid State Commun.* **19**, 1079 (1976).

[12] R. Longuinhos, J. Ribeiro-Soares, *Phys. Chem. Chem. Phys.* **18**, 25401 (2016).

[13] V. Capozzi, *Phys. Rev. B* **23**, 836 (1981).

[14] E. Mooser, M. Schluter, *Nuovo Cim.* **18B**, 164 (1973).

[15] N.C. Fernelius, *Prog. Cryst. Growth Charact.* **28**, 275 (1994).